SIMULATION OF FLUID-STRUCTURE INTERACTION IN BIOMECHANICS USING FOAM-EXTEND

HUA-DONG YAO[1, A)], HÅKAN NILSSON[1, B)], MATS SVENSSON[1], HÅKAN ROOS[2]
[1] *Department of Mechanics and Maritime Sciences, Chalmers University of Technology, Sweden*
[2] *Department of Vascular Surgery, Sahlgrenska University Hospital, Gothenburg, Sweden*
a) huadong.yao@chalmers.se; b) hakan.nilsson@chalmers.se

Keywords: *FSI, Bio-mechanics, Whiplash, EVAR, Stent graft*

Abstract
Fluid-structure interaction (FSI) occurring in two applications in biomechanics is investigated using numerical simulations. One application is the interaction between the dorsal root ganglion and the surrounding fluids (i.e., venous blood and cerebrospinal fluid), and the other application is for the forces and deformation of stent grafts caused by pulsatile blood pressure. In these applications the fluids dynamically interact with the deformable structures. The simulation tool is the FSI package distributed in the Extend-bazaar. The flow and structural deformation are simulated in a segregated way. A strongly coupled partitioned method is used to couple the fluid and structure simulations. The interaction processes of the applications are addressed qualitatively. New insights into the dorsal-root-ganglion injury, which could arise due to whiplash motion, and the forces on stent grafts are gained based on the results. The present FSI solver is considered an effective numerical tool for studying FSI subjects in biomechanics.

Methodology of FSI solver
The open source software FOAM-extend [4] is used together with the FSI package distributed in the Extend-bazaar. Refer to the studies by Jasak [4] and Tuković and Jasak [8] for the details of the governing equations of fluids and structures.
The flow equations are solved based on a second-order finite volume method (FVM) with automatic mesh motion. The PISO (Pressure Implicit Splitting of Operators) algorithm [2] is utilized in the method. A Laplace equation is adopted to govern the automatic mesh motion. A second-order finite element method (FEM) is used to solve this equation [8]. A second-order backward scheme is employed for the time marching.
The structure equations are solved using a second-order cell-centered scheme for the space discretization [8]. A segregated algorithm is used to separately solve the displacement increment vectors. The incomplete Cholesky conjugate gradient iterative solver (ICCG) [3] is employed to compute the system matrix. An implicit second-order three-stage backward scheme is used for the time-marching.
A strongly coupled partitioned method with a Picard iterative process is employed to couple the fluid and structure solvers [5]. The Aitken method [1] is applied to accelerate the convergence speed of the coupling.

Whiplash dorsal root ganglion injury
The dorsal root ganglion (DRG) can be injured during whiplash motion [9]. As shown in Figure 1, the DRG is embedded in the foramen of the cervical vertebra. A possible cause of the injury is that the DRG and dura mater (DM) can be significantly deformed due to impulsive pressure in the surround fluids, i.e., the venous blood and cerebrospinal fluid (CSF).
A geometrical model is established based on the anatomy illustrated in Figure 1. The fluid and structure geometries and corresponding boundary conditions are shown in Figure 2. The FSI is found including pulling and pressing processes, to which the DRG is subjected. The extreme statuses of the processes are shown in Figure 3. The maximum stretched deformation of the DRG is observed at 0.055 s during the pulling, and the maximum compression at 0.1s during the pressing. The deformation interacts with the flows inside and outside the spinal canal. The largest von Mises stress of the DRG is observed near its end. This indicates potential structural damage positions. In addition, the largest pressure gradient is found at the foramen, where the DRG is located at. The figure for this observation is not shown here for the sake of brevity.

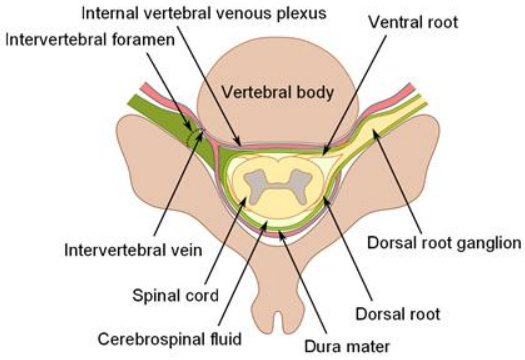

Figure 1: A schematic diagram showing a transverse slice of a vertebra in the mid cervical spine [9].

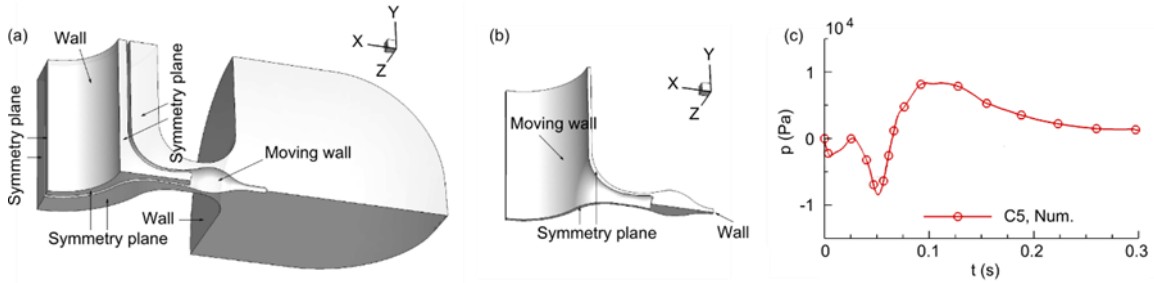

Figure 2: (a) The fluid domain and boundary conditions, (b) the structure domain and boundary conditions, and (c) the transient pressure in the cervical vertebra C5 [9], which is imposed at the inlets of the fluid domain.

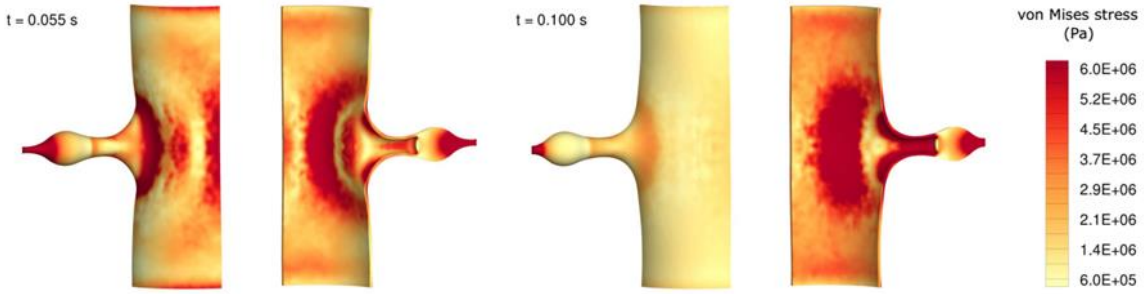

Figure 3: The deformation of the DRG and DM, which is the sheet part of the structure, at 0.055 s and 0.1 s. The contours of the von Mises stress are colored.

Flow-induced forces and deformation of stent grafts

Endovascular aortic repair (EVAR) is a minimal-invasive technique for treating abdominal aortic aneurysms. A stent graft is placed in the aorta through a sheath that is inserted into the aorta through the femoral arteries in the groin. As the sheath is slowly pulled back the stent graft is released and self-expands to fixate to the healthy artery walls at the proximal and distal ends of the aneurysm. An iliac limb stent graft is inserted into the contralateral iliac artery. It self-expands to fixate to the already inserted stent graft in the proximal end and to the iliac artery in the distal end. The stent graft is kept in place by the force exerted on the artery wall due to the self-expansion, and in some cases hooks at the proximal end but not in the connection and at the distal ends. The stent graft thus excludes the aneurysm from the circulation. Long-term EVAR durability is mainly compromised due to leakage into the aneurysm sac which is influenced by stent graft migration at the connections and distal ends, causing potentially lethal leakages. The flow-induced forces have experimentally been shown to have the potential to cause distal end iliac limb stent graft migration [6]. It was shown that the distal displacement forces increase with the magnitude of the pulsatile forces and the angulation, but not with stroke frequency. Roos et al. [7] showed in an extended experimental study that the forces are influenced by the distal stent graft diameter and the shape of the curvature. The experimental studies are however not sufficient to distinguish between the different mechanisms causing the forces, which is why numerical fluid-structure interaction studies are performed in the present work.

Figure 4 shows the tapered, tubular and bell-bottom iliac limb stent graft configurations and numerical results. The straight proximal and distal end sections are rigid fluid regions that separate the flexible stent graft region from the inlet (upper) and outlet (lower). The pulsatile velocity and pressure, determined from the experiments by Roos et al. [7], are set at the inlet and outlet, respectively. Each configuration shows the velocity magnitude (upper left) and the magnified iliac limb stent graft deformation and von Mises stress (lower right). It is shown that large deformations and high displacement forces occur at the distal end, in particular for the bell-bottom configuration. The main cause of the forces is determined

by a comparison with a case without flow, keeping only the pressure pulsations. It can be seen that less than 3% of the forces have their origin in the flow, and the pressure is thus the main cause of the forces. The 90-degree bend of the iliac limb stent graft separates the proximal and distal forces, and the forces are also estimated by calculating the instantaneous values of pressure times cross-section area. This shows that the flexibility of the graft absorbs up to 15% of the forces.

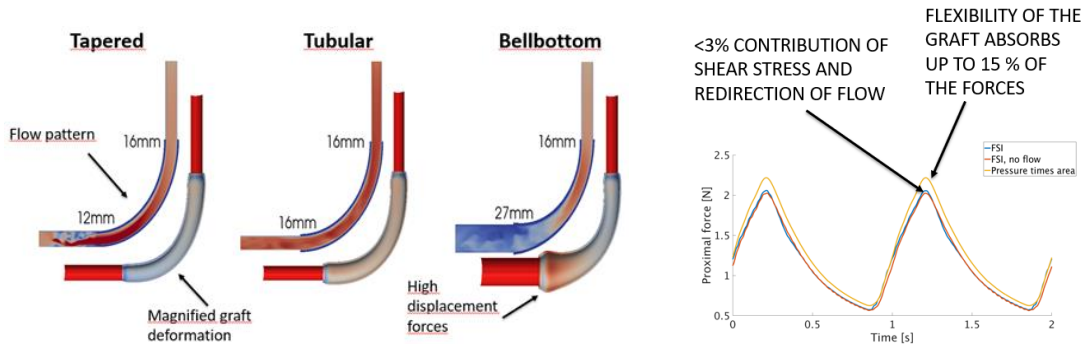

Figure 4: Iliac limb stent graft configurations and numerical results.

Acknowledgements

The present work has been partly funded by the Transport Area of Advance (AoA) of Chalmers University of Technology, Sweden. We appreciate the computer resources provided by the Swedish National Infrastructure for Computing (SNIC). We also thank Prof. Jasak and Prof. Tuković for the FSI code and discussions.

References

[1] Aitken, A., 1926. On bernoulli's numerical solution of algebraic equations. Proceedings of the Royal Society of Edinburgh 46, 289–305.

[2] Issa, R.I., 1986. Solution of the implicitly discretised fluid flow equations by operator-splitting. Journal of Computational Physics 62, 40.

[3] Jacobs, D.A.H., 1980. Preconditioned conjugate gradient methods for solving systems of algebraic equations. Technical Report RD/L/N193/80, Central Electricity Research Laboratories.

[4] Jasak, H., 1996. Error Analysis and Estimation for the Finite Volume Method with Applications to Fluid Flows. Phd thesis. Department of Mechanical Engineering, Imperial College of Science, Technology and Medicine.

[5] Matthies, H., Niekamp, R., Steindorf, J., 2006. Algorithms for strong coupling procedures. Computer Methods in Applied Mechanics and Engineering 195, 2028–2049.

[6] Roos, H., Ghaffari, M., Falkenberg, M., Chernoray, V., Jeppson, A., Nilsson, H., 2014. Eur J Vasc Endovasc Surg (2014) 47, 262-267

[7] Roos, H., Tokarev, M., Chernoray, V., Ghaffari, M., Falkenberg, M., Jeppson, A., Nilsson, H., 2016. Displacement Forces in Stent Grafts: Influence of Diameter Variation and Curvature Asymmetry. Eur J Vasc Endovasc Surg (2016) 52, 150-156

[8] Tuković Ž., Jasak, H., 2007. Updated lagrangian finite volume solver for large deformation dynamic response of elastic body. Transactions of FAMENA 31(1), 55.

[9] Yao, H.D., Svensson, M.Y., Nilsson, H., 2016. Transient pressure changes in the vertebral canal during whiplash motion a hydrodynamic modeling approach. Journal of Biomechanics 49 (3), 416–422.